Dynamic Control of Human Eye on Head System

Bijoy K. Ghosh[1], Indika B. Wijayasinghe[1]
1. Laboratory for BioCybernetics and Intelligent Systems, Texas Tech University, Lubbock, Texas, USA
E-mail: {bijoy.ghosh, indika.wijayasinghe}@ttu.edu

Abstract: In this paper we study the human eye movement, when the eye shifts its gaze between two possible gaze directions, as a simple mechanical control system. When the head is restrained to remain fixed, eye movements obey Listing's constraint, which states that the allowed orientations of the eye are obtained by rotating a fixed 'primary gaze direction' by a subclass of rotation matrices. These rotation matrices have their axes of rotation restricted to a fixed plane perpendicular to the primary gaze direction. Under head fixed restriction, eye movement satisfies the Listing's constraint throughout its entire trajectory. On the other hand, when the head is allowed to move, the eye orientations satisfy the Listing's constraint only at the beginning and at the end of a trajectory. Intermediate points of the trajectory, do not satisfy the Listing's constraint. In this paper, we study the dynamic control of eye movement with or without satisfaction of the Listing's constraint. The control has been synthesized by a suitable choice of a potential function and an externally added damping term.

Key Words: Eye Movement, Listing's Law, Euler Lagrange Equation, Head Fixed, Head Free

1 INTRODUCTION

Modeling the eye, in order to generate various eye movements, has been one of the important goals among neurologists, physiologists and engineers since 1845 (e.g. see the work of Listing, Donders and Helmoltz etc in [21], [9]). Previous studies which used modeling as a means of understanding the control of the eye movements have adopted two main approaches. One focusing on the details of the properties of the EOMs [13], [15] and the other focusing on the control mechanisms using oversimplified linear models with all the details of the above EOM properties ignored but focusing on the information processing and control aspects [18], [20]. In spite of several notable studies of three dimensional eye movements [3], [8] and many others, with the exception of some recent papers in the subject [17], [24], there has not been a rigorous treatment of the topic in the framework of modern control theory and geometric mechanics. Assuming the eye to be a rigid sphere, the problem of eye movement can be treated as a mechanical control system [5], [16] and the results of classical mechanics can be promptly applied.

Most of the earlier studies in eye movement assumed that the head remained fixed and the eye is allowed to move freely. It was observed by Listing (see [22]), that in this situation the orientation of the eye was completely determined by its gaze direction. Subsequently it was shown that starting from a frontal gaze, any other gaze direction is obtained by a rotation matrix whose axis of rotation is constrained to lie on a plane, called the Listing's Plane. Consequently, the set of all orientations the eye can assume is a submanifold of $\mathbf{SO}(3)$ (see Boothby [4] for a definition) called **LIST**. Listing showed that in a head fixed environment, eye orientations are restricted to this specific submanifold **LIST**.

This material is based upon work supported in part by the National Science Foundation under Grant No. 0523983. Any opinions, findings, and conclusions or recommendations expressed in this material are those of the author(s) and do not necessarily reflect the views of the National Science Foundation.

In this paper, we are interested in the study of eye movement when head is allowed to move as well. To fix our ideas, assume that the head can move spontaneously on the torso and the eye moves with respect to the head coordinate. Assume that our goal is to fixate on a stationary target on the visual space observed at a certain angle from the initial gaze direction. In this situation, as was described by Tweed [23], the eye moves rapidly towards the target, violating the Listing's constraint. However, even under this motion, the initial and the final orientation of the eye is on the submanifold **LIST**. The head, in the mean time, moves spontaneously towards the object as well, following a Listing like constraint that goes by the name Donders' constraint [14], [19] and [23]. Study of head movement satisfying the Donders' constraint is a subject of our future research and will be reported elsewhere.

Simultaneous movement of the eye and the head to fixate on a target, either stationary or moving, is a subject of intense research (see [6], [11]) in recent years. In order to stabilize a target on the retina under head movement, the eyes have to be controlled by the vestibulo-ocular (VOR) reflex [2], [12]. In this paper, we do not discuss the VOR reflex explicitly as a control problem. Starting from a suitable Riemannian metric, we write down the dynamics of the eye movement problem when the Listing's constraint is satisfied and when it is not. As we have already argued, both of these cases are important – one in which the head is fixed and the other when the head is not. The basic approach in this paper is an extension of our earlier paper [17], which involves writing down the dynamical systems using the Euler Lagrange equation. We would also like to refer our readers to a recent paper [10] on the optimal control of gaze shift.

2 QUATERNIONIC REPRESENTATIONS

Representation of 'eye orientation' using quaternion has already been described in [17]. For the sake of clarity, we revisit some of the main ideas in this section. A quaternion is a four tuple of real numbers denoted by Q. We write each element $a \in Q$ as

$$a = a_0\, 1 + a_1\, i + a_2\, j + a_3\, k, \qquad (1)$$

and call $a_1\ i + a_2\ j + a_3\ k$ its vector part and $a_0\ 1$ its scalar part. The vector part is identified with the vector (a_1, a_2, a_3) and the scalar part is written simply as a_0. It is natural to define the map

$$vec\ :\ Q\ \rightarrow\ \mathbb{R}^3,\ \text{where}\ a\ \mapsto\ (a_1, a_2, a_3). \tag{2}$$

The space of unit quaternion is identified with the unit sphere in $\mathbb{R}^4$ and denoted by S^3. Each $q\ \in\ S^3$ can be written as

$$q\ =\ \cos\frac{\phi}{2}\ 1\ +\ \sin\frac{\phi}{2}\ n_1\ i\ +\ \sin\frac{\phi}{2}\ n_2\ j\ +\ \sin\frac{\phi}{2}\ n_3\ k, \tag{3}$$

where $\phi\ \in\ [0, 2\pi]$, and $n\ =\ (n_1, n_2, n_3)$ is a unit vector in $\mathbb{R}^3$. If q is an unit quaternion represented as in (3), one can show the following using simple properties of quaternion multiplication –

"The vector $vec[q\ \bullet\ (v_1\ i\ +\ v_2\ j\ +v_3\ k)\ \bullet q^{-1}]$ **is rotation of the vector** (v_1, v_2, v_3) **around the axis** n **by a counterclockwise angle** ϕ**."**

If S^3 is the space of unit quaternions, we define a map between S^3 and $SO(3)$ described as follows

$$rot\ :\ S^3\ \rightarrow\ SO(3) \tag{4}$$

where

$$q\ =\ \begin{pmatrix} q_0 \\ q_1 \\ q_2 \\ q_3 \end{pmatrix}\ \longmapsto \tag{5}$$

$$\begin{pmatrix} q_0^2+q_1^2-q_2^2-q_3^2 & 2(q_1q_2-q_0q_3) & 2(q_1q_3+q_0q_2) \\ 2(q_1q_2+q_0q_3) & q_0^2+q_2^2-q_1^2-q_3^2 & 2(q_2q_3-q_0q_1) \\ 2(q_1q_3-q_0q_2) & 2(q_2q_3+q_0q_1) & q_0^2+q_3^2-q_1^2-q_2^2 \end{pmatrix}.$$

Recall that $SO(3)$ is the space of all 3×3 matrices W such that $WW^T\ =\ I$, the identity matrix and $det\ W\ =\ 1$. It can be verified, perhaps not so easily, that for any nonzero vector v in $\mathbb{R}^3$ we have

$$rot(q)\ v\ =\ vec[q \bullet v \bullet q^{-1}].$$

Note that the map 'rot' in (4) is surjective but not $1-1$. This is because both q and $-q$ in S^3 has the same image. We now write down a parametrization of the unit vector 'n' in (3) as

$$n\ =\ \begin{pmatrix} \cos\theta\ \cos\alpha \\ \sin\theta\ \cos\alpha \\ \sin\alpha \end{pmatrix}. \tag{6}$$

Combining (3) and (6), we have the following parametrization of unit quaternions

$$q\ =\ \begin{pmatrix} \cos\frac{\phi}{2} \\ \sin\frac{\phi}{2}\cos\theta\ \cos\alpha \\ \sin\frac{\phi}{2}\sin\theta\ \cos\alpha \\ \sin\frac{\phi}{2}\sin\alpha \end{pmatrix}. \tag{7}$$

Using the coordinates (θ, ϕ, α) we have the following sequence of maps

$$[0,\pi]\ \times\ [0,2\pi]\ \times\ [-\frac{\pi}{2}, \frac{\pi}{2}]\ \xrightarrow{\ \rho\ }\ S^3\ \xrightarrow{\ rot\ }\ SO(3)\ \xrightarrow{\ proj\ }\ S^2, \tag{8}$$

where

$$\rho(\theta, \phi, \alpha)\ =\ q\ \ (\text{in}\ (7)),$$
$$rot(q)\ =\ W$$

and

$$proj(W)\ =\ \begin{pmatrix} \sin\theta\ \sin\phi\ \cos\alpha\ +\ \cos\theta\ \sin^2\frac{\phi}{2}\ \sin 2\alpha \\ -\cos\theta\ \sin\phi\ \cos\alpha\ +\ \sin\theta\ \sin^2\frac{\phi}{2}\ \sin 2\alpha \\ \cos^2\frac{\phi}{2}\ -\ \sin^2\frac{\phi}{2}\ \cos 2\alpha \end{pmatrix}. \tag{9}$$

The matrix W in $SO(3)$ can be easily written from (5) and has been omitted. The points in S^2 described by (9) provide a description of the gaze directions as a function of the coordinate angles θ, ϕ, α with respect to an initial gaze direction of $(0,0,1)^T$, i.e. obtained by rotating the vector $(0,0,1)^T$ using the rotation matrix W.

3 EYE ORIENTATIONS SATISFYING LISTING'S CONSTRAINT

Listing's law asserts that the axis of rotation 'n' in (6) is restricted to a plane. We shall describe this plane by restricting $\alpha\ =\ 0$ and obtain $n\ =\ (\cos\theta,\ \sin\theta,\ 0)^T$, $q\ =\ (\cos\frac{\phi}{2},\ \sin\frac{\phi}{2}\ \cos\theta,\ \sin\frac{\phi}{2}\ \sin\theta,\ 0)^T$ and the matrix W given by

$$\begin{pmatrix} \cos^2\frac{\phi}{2}+\cos 2\theta\ \sin^2\frac{\phi}{2} & \sin 2\theta\ \sin^2\frac{\phi}{2} & \sin\theta\ \sin\phi \\ \sin 2\theta\ \sin^2\frac{\phi}{2} & \cos^2\frac{\phi}{2}-\cos 2\theta\ \sin^2\frac{\phi}{2} & -\cos\theta\ \sin\phi \\ -\sin\theta\ \sin\phi & \cos\theta\ \sin\phi & \cos\phi \end{pmatrix}. \tag{10}$$

Under the Listing's constraint, we define **LIST** to be the associated submanifold of $\mathbf{S}^3$ and $\mathbf{SO}_L(3)$ to be the associated submanifold of **SO(3)**. They are both two dimensional submanifolds parameterizing the rotation in $\mathbf{S}^3$ and $\mathbf{SO}_L(3)$ respectively. The gaze direction $(0,\ 0,\ 1)^T$ is transformed to the direction $(\sin\theta\ \sin\phi,\ -\cos\theta\ \sin\phi,\ \cos\phi)^T$ by the rotation matrix (10).

Listing's constraint is a restriction on the axis of rotation, for gaze transitions away from the primary gaze direction. It can be easily checked that the submanifold $\mathbf{SO}_L(3)$ is not a subgroup of **SO(3)** and hence matrix product of two elements of $\mathbf{SO}_L(3)$ would not necessarily be an element of $\mathbf{SO}_L(3)$. What this means is that *gaze transition between a secondary position and a tertiary position, i.e. away from the primary position,* is not necessarily taking place with an axis of rotation on the Listing's plane.

During transition between two arbitrary gaze directions when the head is assumed to be fixed, Listing's law is to be viewed as a constraint on the instantaneous orientations of the eye, in particular the orientations are restricted to remain inside $\mathbf{SO}_L(3)$ at all times. What complicates this picture is that when the head is allowed to move, the eye orientations are allowed to escape $\mathbf{SO}_L(3)$ during transition between two points on $\mathbf{SO}_L(3)$.

4 RIEMANNIAN METRIC ON SO(3) AND LIST

It has been described in [17] that eye rotations are typically confined to a sub manifold **LIST** of $\mathbf{SO}(3)$ especially when the head is restrained to be fixed. In order to write down the equations of motion, one needs to know the kinetic and the potential energies of the eye in motion. The kinetic energy is given by the induced Riemannian metric on **LIST**, induced from the Riemannian metric on $\mathbf{SO}(3)$. The Riemannian metric is derived from the moment of inertia of the

eye ball. We assume that the eye is a perfect sphere and its inertia tensor is equal to $I_{3\times 3}$. This is associated with a left invariant Riemannian metric on $\mathbf{SO}(3)$ given by

$$< \Omega(e_i), \Omega(e_j) >_I = \delta_{i,j}, \tag{11}$$

where

$$\Omega(e_k) = \begin{pmatrix} 0 & \delta_{3,k} & -\delta_{2,k} \\ -\delta_{3,k} & 0 & \delta_{1,k} \\ \delta_{2,k} & -\delta_{1,k} & 0 \end{pmatrix} \tag{12}$$

and $\delta_{l,m}$ denotes the Kronecker delta function. An easy way to carry out computation using this Riemannian metric is provided by an isometric submersion **rot** between $\mathbf{S}^3$ and $\mathbf{SO}(3)$ already described in (4) and (8).

The composition mapping $\mathbf{rot} \circ \rho(\theta, \phi, \alpha)$ is a rotation around the axis (6) by a counterclockwise angle ϕ. Note in particular that when $\alpha = 0$, the axis of rotation is restricted to a plane, known as the Listing's plane. The angle θ measures the angle of the axis on the Listing's plane and the angle α measures deviation of the axis from the Listing's Plane. In order to compute the Riemannian Metric on $\mathbf{SO}(3)$, we write

$$\rho_*\left(\frac{\partial}{\partial\theta}\right) = \begin{pmatrix} 0 \\ -\sin(\phi/2)\ \sin(\theta)\ \cos(\alpha) \\ \sin(\phi/2)\ \cos(\theta)\ \cos(\alpha) \\ 0 \end{pmatrix}; \tag{13}$$

$$\rho_*\left(\frac{\partial}{\partial\alpha}\right) = \begin{pmatrix} 0 \\ -\sin(\phi/2)\ \cos(\theta)\ \sin(\alpha) \\ -\sin(\phi/2)\ \sin(\theta)\ \sin(\alpha) \\ \sin(\phi/2)\ \cos(\alpha) \end{pmatrix}; \tag{14}$$

$$\rho_*\left(\frac{\partial}{\partial\phi}\right) = \begin{pmatrix} -\frac{1}{2}\sin(\phi/2) \\ \frac{1}{2}\cos(\phi/2)\ \cos(\theta)\ \cos(\alpha) \\ \frac{1}{2}\cos(\phi/2)\ \sin(\theta)\ \cos(\alpha) \\ \frac{1}{2}\cos(\phi/2)\ \sin(\alpha) \end{pmatrix}. \tag{15}$$

Then we obtain the inner products given by,

$$\begin{aligned} g_{11} &= \langle\frac{\partial}{\partial\theta}, \frac{\partial}{\partial\theta}\rangle = \sin^2(\phi/2)\cos^2(\alpha) \\ g_{22} &= \langle\frac{\partial}{\partial\alpha}, \frac{\partial}{\partial\alpha}\rangle = \sin^2(\phi/2) \\ g_{33} &= \langle\frac{\partial}{\partial\phi}, \frac{\partial}{\partial\phi}\rangle = \frac{1}{4} \\ \text{and } g_{ij} &= 0 \text{ for } i \neq j \text{ with } i, j = 1, 2, 3. \end{aligned} \tag{16}$$

The Riemannian metric on $\mathbf{SO}(3)$ is given by:

$$g = \sin^2(\phi/2)\cos^2(\alpha)\, d\theta^2 + \sin^2(\phi/2)\, d\alpha^2 + \frac{1}{4} d\phi^2. \tag{17}$$

Note that restricted to the Listing's plane, i.e. when $\alpha = 0$, the Riemannian metric on **LIST** is given by

$$g = \sin^2(\phi/2)\, d\theta^2 + \frac{1}{4} d\phi^2 \tag{18}$$

as has been already described in [17].

Using the Riemannian metric (17) for $\mathbf{SO}(3)$, it is a straightforward but tedious computation to show that the associated geodesic equation is given by

$$\begin{aligned} \ddot{\theta} + \dot{\theta}\dot{\phi}\cot(\phi/2) - 2\dot{\theta}\dot{\alpha}\tan(\alpha) &= 0 \\ \ddot{\phi} - (\dot{\theta})^2 \sin(\phi)\cos^2(\alpha) - (\dot{\alpha})^2 \sin(\phi) &= 0 \\ \ddot{\alpha} + \frac{1}{2}(\dot{\theta})^2 \sin(2\alpha) + \dot{\phi}\dot{\alpha}\cot(\phi/2) &= 0. \end{aligned} \tag{19}$$

When $\alpha = 0$, the above geodesic equation (19) reduces to the following pair of equations already described in [17] given by

$$\begin{aligned} \ddot{\theta} + \dot{\theta}\dot{\phi}\cot(\phi/2) &= 0 \\ \ddot{\phi} - (\dot{\theta})^2 \sin(\phi) &= 0. \end{aligned} \tag{20}$$

The geodesic equation (20) can also be directly computed from the Riemannian metric (18) on the submanifold **LIST** of $\mathbf{SO}(3)$.

5 GENERAL EQUATION OF MOTION

The Riemannian Metrics that we had obtained so far in (17) and (18) enables us to write down an expression for the kinetic energy KE. In general, the dynamics is affected by an additional potential energy and an external input torque. Let us consider a general form of the potential function given by

$$V(\theta, \phi, \alpha) = A \sin^2\frac{\phi}{2} + B \cos^2\frac{\phi}{2} \sin^2\alpha. \tag{21}$$

The expression for the Lagrangian is given by

$$L = KE - V, \tag{22}$$

and the equation of motion is described by

$$\frac{d}{dt}\left(\frac{\partial L}{\partial\dot{\beta}}\right) - \left(\frac{\partial L}{\partial\beta}\right) = \tau_\beta \tag{23}$$

where β is the angle variable.

5.1 Motion satisfying the Listing's Constraint

The Listing's constraint is satisfied when $\alpha = 0$ and the kinetic energy is given by

$$KE = \frac{1}{2}\left[\sin^2\frac{\phi}{2}\dot{\theta}^2 + \frac{1}{4}\dot{\phi}^2\right].$$

The following motion equation follows easily from the Euler-Lagrange equation given by

$$\begin{aligned} \ddot{\theta} + \dot{\theta}\dot{\phi}\cot(\phi/2) &= \csc^2(\phi/2)\,\tau_\theta \\ \ddot{\phi} - (\dot{\theta})^2 \sin(\phi) &+ 2\mathrm{A}\sin(\phi) = 4\tau_\phi. \end{aligned} \tag{24}$$

5.2 Motion that does not satisfy the Listing's Constraint

When α is unrestricted, Listing constraint is not satisfied and the rotation matrix remains unrestricted in $\mathbf{SO}(3)$. In this case, the kinetic energy is given by

$$KE = \frac{1}{2}\left[\sin^2\frac{\phi}{2}\cos^2\alpha\dot{\theta}^2 + \sin^2\frac{\phi}{2}\dot{\alpha}^2 + \frac{1}{4}\dot{\phi}^2\right]. \tag{25}$$

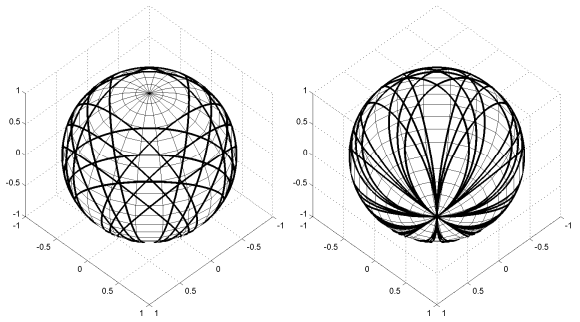

(a) Front (b) Back

Fig. 1: Geodesic curves from (20) plotted on the gaze space. Geodesics are circular passing through the backward gaze

One can now obtain the following equation from the Euler Lagrange's equation.

$$\begin{aligned}
\ddot{\theta} &= 2\tan\alpha\,\dot{\alpha}\,\dot{\theta} - \dot{\theta}\,\dot{\phi}\cot\frac{\phi}{2} + \csc^2\frac{\phi}{2}\sec^2\alpha\,\tau_\theta \\
\ddot{\phi} &= \sin\phi\left[\cos^2\alpha\,\dot{\theta}^2 + \dot{\alpha}^2 - 2A\right] \\
&\quad + 4B\sin\phi\,\sin^2\alpha + 4\,\tau_\phi \\
\ddot{\alpha} &= -\cot\frac{\phi}{2}\,\dot{\alpha}\,\dot{\phi} - \frac{1}{2}\sin(2\alpha)\,\dot{\theta}^2 \\
&\quad + \left[\tau_\alpha - B\cos^2\frac{\phi}{2}\sin(2\alpha)\right]\csc^2\frac{\phi}{2}. \qquad (26)
\end{aligned}$$

6 SOME SIMULATIONS ON GEODESIC AND MOTION EQUATION

In this section we show via simulation, some of the geodesic trajectories and solutions to the motion equation under a suitable choice of potential energy and the input torque.

Example 1: In this example we solve the geodesic equation (20) (corresponds to eye rotation that satisfy the Listing's constraint) and show in Fig. 1 that the geodesic curves are circles passing through a fixed point. In Fig. 1 we have plotted the gaze directions as a function of time starting from different initial conditions. In plotting the figure, we have chosen the convention that the identity rotation matrix corresponds to the frontal gaze. Our simulations show that all geodesics are circles that pass through the backward gaze.

Example 2: In this example we solve the motion equation (24) (corresponds to eye rotation that satisfy the Listing's constraint) and show the gaze trajectories in Fig. 2. We have assumed $\tau_\theta = \tau_\phi = 0$, and increasing magnitudes A of the potential function has been chosen. Our simulations show that with increasing magnitude of the potential function, the gaze trajectories are restricted to a smaller neighborhood of $\phi = 0$, the frontal gaze.

Example 3: We remark that in example 2, one of the properties of the eye movement trajectory is that with increasing magnitude A of the potential function the gaze trajectories are restricted to the frontal part of the visual field, a desirable feature. Unfortunately, we observe that the trajectories themselves are increasingly jittery. In this

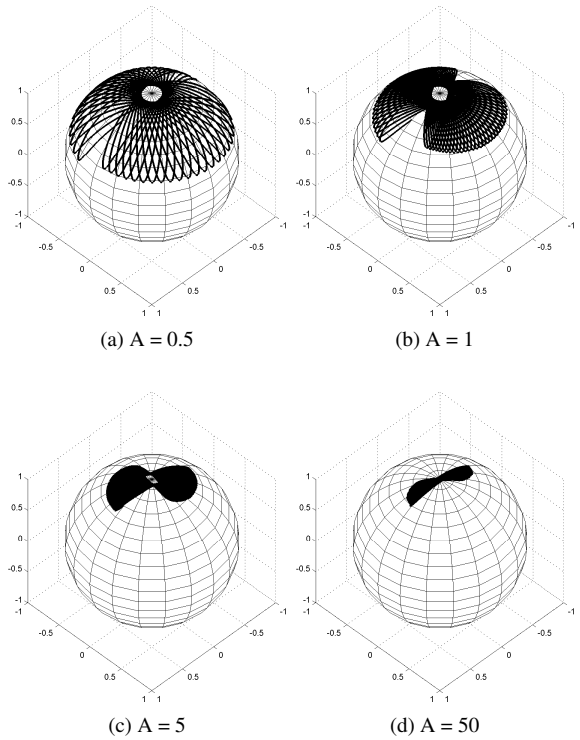

(a) A = 0.5 (b) A = 1

(c) A = 5 (d) A = 50

Fig. 2: Gaze motion from (24) with the external control set to zero, i.e. $\tau_\theta = \tau_\phi = 0$. Increasing magnitude A of the potential function shows that the eye movements are restricted to the frontal gaze.

example we repeat example 2 but choose $\tau_\theta = -k\,\dot{\theta}$ and $\tau_\phi = -k\,\dot{\phi}$ in order to dampen the fluctuations in the trajectories. The results are plotted in Fig. 3.

Example 4: In this example we repeat example 3, but this time the potential function has a minimum at an arbitrary final gaze direction (given by θ_f, ϕ_f), away from the frontal gaze. This is achieved by choosing the potential function

$$V(\theta,\phi) = A\,[\sin^2\frac{\phi-\phi_f}{2} + \sin^2\frac{\theta-\theta_f}{2}]. \qquad (27)$$

The results are plotted in Fig. 4. The plots are quite similar to that of Fig. 3 except that the terminal points are different.

Example 5: In this example we solve the geodesic equation (19) (corresponds to eye rotation that does not satisfy the Listing's constraint). We show in Fig. 5 that the projection of the geodesic curves on the gaze space are circles that do not necessarily pass through a fixed point. Fig. 5a and Fig. 5b are two cases of the simulation assuming different initial conditions for $\dot{\alpha}$. Each figure consists of curves with different initial choices of θ and ϕ.

Example 6: In this example we solve the motion equation (26) (corresponds to eye rotation that does not satisfy the Listing's constraint) and show the gaze trajectories in Fig. 6. We have assumed $\tau_\theta = \tau_\phi = \tau_\alpha = 0$, the parameters A and B are chosen to be equal and increasing magnitudes A of the potential function (21) has been chosen. Our simulations show that with increasing magnitude of the

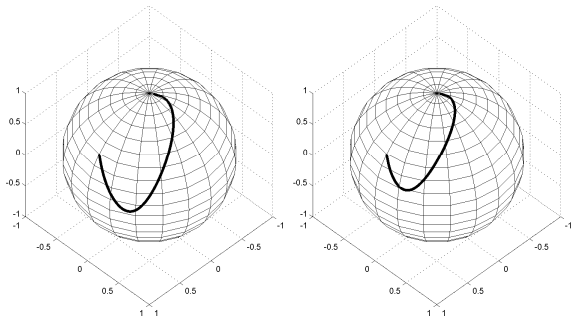

(a) A = 0.5 (b) A = 1

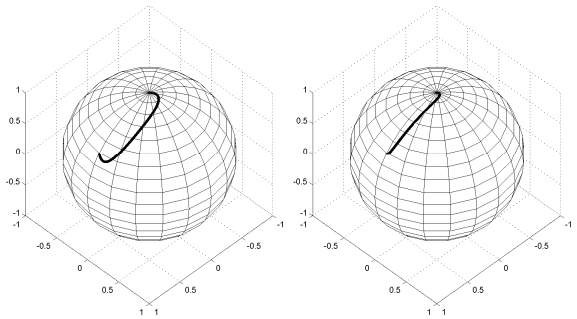

(c) A = 5 (d) A = 50

Fig. 3: Gaze motion for (24) with a damping term $\tau_\theta = -0.1\,\dot{\theta}$ and $\tau_\phi = -0.1\,\dot{\phi}$. The gaze converges smoothly to the point of zero potential, viz. the frontal gaze direction.

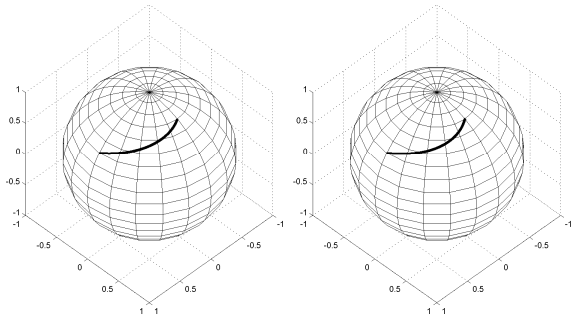

(a) A = 0.5 (b) A = 1

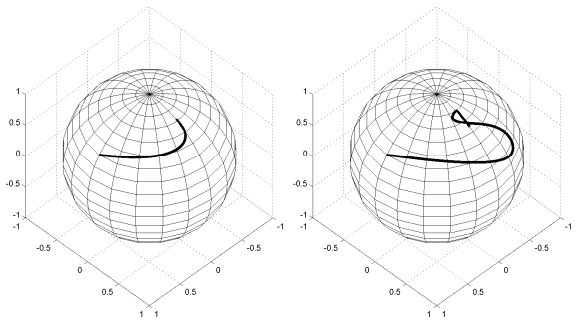

(c) A = 5 (d) A = 50

Fig. 4: Gaze motion obtained by changing the potential function to (27). With a damping term set to $\tau_\theta = -1.0\,\dot{\theta}$ and $\tau_\phi = -1.0\,\dot{\phi}$, the gaze converges smoothly to an arbitrary a priory chosen gaze direction.

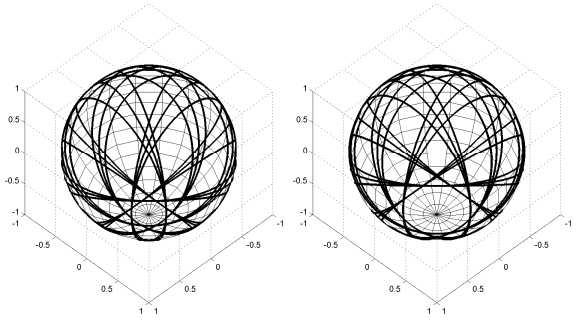

(a) (b)

Fig. 5: Projection of the geodesic curves for (19) on the gaze space. As opposed to what we found in Fig. 1, each projection is a circle that do not pass through one fixed gaze

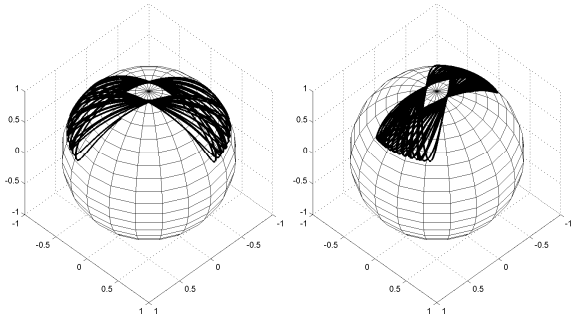

(a) A = 0.5 (b) A = 1

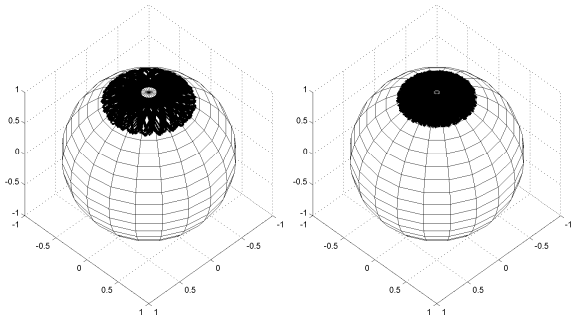

(c) A = 5 (d) A = 50

Fig. 6: Gaze motion from (26) with the external control set to zero, i.e. $\tau_\theta = \tau_\phi = \tau_\alpha = 0$. Choosing $A = B$, and increasing the magnitude of the parameter A of the potential function (21) shows that the eye movements are restricted to the frontal gaze.

potential function, the gaze trajectories are restricted to a smaller neighborhood of $\phi = 0$ and $\alpha = 0$, the frontal gaze that satisfies the Listing's constraint. Note once again that without the damping term, the eye movements are oscillatory.

Example 7: In this last example, we solve an equation analogous to the motion equation (26) by assuming a potential function of the form

$$V(\theta,\phi,\alpha) = 1.0\,[\sin^2\frac{\phi-\phi_f}{2} + \sin^2\frac{\theta-\theta_f}{2} + \sin^2\frac{\alpha-\alpha_f}{2}]. \tag{28}$$

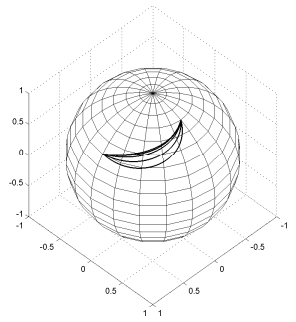

(a) Front

Fig. 7: Gaze trajectories that start and end at the same point on the gaze space. Points of the trajectories, except perhaps the initial point, do not satisfy the Listing's constraint.

A damping term has been added with the constant $k = 1.0$. In Fig. 7, the projection of the eye trajectory on the gaze space has been plotted. All trajectories start from a fixed point on the Listing's submanifold **LIST** and end at different points in $\mathbf{SO}(3)$ with the property that the projection of the end points on the gaze space is a fixed point. In other words, the gaze trajectories start and end at the same point but the final orientation of the eye differs for different choices of α_f. It has been observed (but not detailed here) that the minimum time and the minimum distance trajectory correspond to a non zero value of α_f, indicating that for minimum time or minimum distance eye movements, it pays to violate the Listing's constraint.

7 SUMMARY, CONCLUSION AND FUTURE RESEARCH

In this paper we have outlined how motion equations can be written starting from a suitable Riemannian Metric and writing down the corresponding Euler Lagrange equations. In particular, these metrics were written down for $\mathbf{SO}(3)$ and one of its important submanifold **LIST**. Writing down the corresponding Euler Lagrange equation is a standard problem in Classical Mechanics (see Abraham and Marsden [1]). In this study, gaze has been actuated by a suitable choice of a potential function. The oscillatory response of the gaze was damped by adding a damping term. An important observation of this paper is that within the class of eye movement dynamics considered, satisfaction of the Listing's constraint comes with a price, both in terms of distance and time. If the goal is to transfer between two gaze points, it is quicker and shorter to violate the Listing's constraint. We have observed, but not discussed in this paper, that the motion equations obtained have points of singularity. Details on this will be discussed in a future paper [7].

REFERENCES

[1] Abraham, R., Marsden, J. E., *Foundations of Mechanics*, AMS Chelsea Publishing, American Mathematical Society, Providence, Rhode Island, 1978.

[2] Angelaki, D., "Eyes on Target: What Neurons Must Do For The Vestibuloocular Reflex During Linear Motion", *J. Neurophysiol.*, vol. 92, pp. 20–35, 2004.

[3] Angelaki, D. and Hess, B. J. M., "Control of Eye Orientation: Where Does the Brain's Role End and the Muscle's Begin", Review Article, *European J. of Neuroscience*, vol. 19, pp. 1–10, 2004.

[4] Boothby, W. M., *An Introduction to Differentiable Manifolds and Riemannian Geometry*, CA: Academic-Press, 1986.

[5] Bullo, F. and Lewis, A. D., *Geometric Control of Mechanical Systems*, Springer-Verlag, 2004.

[6] Crawford, J. D., Ceylan, M. Z., Klier, E. M. and Guitton, D., "Three Dimensional Eye-Head Coordination During Gaze Saccades in the Primate", *J. Neurophysiol.*, vol. 81, pp. 1760–1782, 1999.

[7] Ghosh, B. K. and Wijayasinghe, I. B., "Geometric Control of Human Eye Under Head Fixed and Head Free Constraints", *IEEE Transactions in Automatic Control*, (to be submitted).

[8] Glasauer, S., "Current Models of the Ocular Motor System", *Neuro-Ophthalmology, Dev. Ophthalmology*, Basel, Karger, vol. 40, pp. 158–174, 2007.

[9] von Helmholtz, H., *Handbuch der Physiologischen Optik.* Hamburg: Vos., 1867.

[10] Kardamakis, A. A., "Optimal Control of Gaze Shifts", *The Journal of Neuroscience*, vol. 29(24), pp. 7723–7730, 2009.

[11] Klier, E. M., Wang, H. and Crawford, D., "Neural Mechanisms of Three-Dimensional Eye and Head Movements", *Ann. N. Y. Acad. Sci.*, vol. 956, pp. 512–514, 2002.

[12] Lehnen, N., Buttner, U. and Glasauer, S., "Vestibular Guidance of Active Head Movements", *Exp. Brain Res.*, vol. 194, pp. 495–503, 2009.

[13] Martin, C. and Schovanec, L., "Muscle Mechanics and Dynamics of Ocular Motion", *J. of Mathematical Systems, Estimation and Control*, vol. 8, pp. 1–15, 1998.

[14] Medendorp, W. P., Gisbergen, J. A. M. Van., Horstink, M. W. I. M. and Gielen, C. C. A. M., "Donders' Law in Torticollis", *J. Neurophysiology*, vol. 82, pp. 2833–2838, 1999.

[15] Miller, J. and Robinson, D., "A Model of the Mechanics of Binocular Alignment", *Computers and Biomedical Research*, vol. 17, pp. 436–470, 1984.

[16] Murray, R. M., "Nonlinear Control of Mechanical Systems: A Lagrangian Perspective", *Annu. Rev. Control*, vol. 21, pp. 31–45, 1997.

[17] Polpitiya, A. D., Dayawansa, W. P., Martin, C. F., and Ghosh, B. K., "Geometry and Control of Human Eye Movements", *IEEE Transactions in Automatic Control*, vol. 52, no. 2, pp. 170–180, Feb. 2007.

[18] Quaia, C. and Optican, L., "Commutative Saccadic Generator is Sufficient to Control a 3D Ocular Plant with Pulleys", *J. Neurophysiol.*, vol. 79, pp. 3197–3215, 1998.

[19] Radau, P., Tweed, D. and Vilis, T., "Three Dimensional Eye head and Chest Orientations Following Large Gaze Shifts and the Underlying Neural Strategies", *J. Neurophysiol.*, vol. 72, pp. 2840–2852, 1994.

[20] Raphan, T., "Modeling Control of Eye Orientation in Three Dimension – Role of Muscle Pulleys in Determining Saccadic Trajectory", *J. Physiol.*, vol. 79, pp. 2653–2667, 1998.

[21] Robinson, D., "The Mechanics of Human Saccadic Eye Movement", *J. Physiol.*, vol. 174, pp. 245–264, 1964.

[22] Tweed, D. and Villis, T., "Geometric Relations of Eye Position and Velocity Vectors During Saccades ", *Vision Res.*, vol. 30, pp. 111–127, 1990.

[23] Tweed, D., "Three Dimensional Model of the human Eye-Head Saccadic System", *J. Neurophysiology*, vol. 77, pp. 654–666, 1997.

[24] Tweed, D., Haslwanter, T. and Fetter, M., "Optimizing Gaze Control in Three Dimensions", *Science*, vol. 281(28), pp. 1363–1365, Aug., 1998.